Airy-soliton interactions in Kerr media

Amitay Rudnick and Dan M. Marom*

Department of Applied Physics, Hebrew University of Jerusalem, Jerusalem, 91904, Israel
**danmarom@cc.huji.ac.il*

Abstract: We investigate and analyze temporal soliton interactions with a dispersive truncated Airy pulse traveling in a nonlinear fiber at the same center wavelength (or frequency), via split step Fourier numerical simulation. Truncated Airy pulses, which remain self-similar during propagation and have a ballistic trajectory in the retarded time frame, can interact with a nearby soliton by its accelerating wavefront property. We find by tracking the fundamental parameters of the emergent soliton—time position, amplitude, phase and frequency—that they alter due to the primary collision with the Airy main lobe and the continuous co-propagation with the dispersed Airy background. These interactions are found to resemble coherent interactions when the initial time separation is small and incoherent at others. This is due to spectral content repositioning within the Airy pulse, changing the nature of interaction from coherent to incoherent. Following the collision, the soliton intensity oscillates as it relaxes. The initial parameters of the Airy pulse such as initial phase, amplitude and time position are varied to better understand the nature of the interactions.

OCIS codes: (190.0190) Nonlinear optics; (190.3270) Kerr effect; (060.5530) Pulse propagation and temporal solitons.

References and links

1. M. V. Berry and N. L. Balazs, "Nonspreading wave packets," Am. J. Phys. **47**(3), 264–267 (1979).
2. J. Durnin, "Exact solutions for nondiffracting beams. I. The scalar theory," J. Opt. Soc. Am. A **4**(4), 651–654 (1987).
3. J. Durnin, J. J. Miceli, Jr., and J. H. Eberly, "Diffraction-free beams," Phys. Rev. Lett. **58**(15), 1499–1501 (1987).
4. G. A. Siviloglou and D. N. Christodoulides, "Accelerating finite energy Airy beams," Opt. Lett. **32**(8), 979–981 (2007).
5. G. A. Siviloglou, J. Broky, A. Dogariu, and D. N. Christodoulides, "Observation of accelerating Airy beams," Phys. Rev. Lett. **99**(21), 213901 (2007).
6. G. A. Siviloglou, J. Broky, A. Dogariu, and D. N. Christodoulides, "Ballistic dynamics of Airy beams," Opt. Lett. **33**(3), 207–209 (2008).
7. P. Polynkin, M. Kolesik, J. V. Moloney, G. A. Siviloglou, and D. N. Christodoulides, "Curved plasma channel generation using ultraintense Airy beams," Science **324**(5924), 229–232 (2009).
8. J. Baumgartl, M. Mazilu, and K. Dholakia, "Optically mediated particle clearing using Airy wavepackets," Nat. Photonics **2**(11), 675–678 (2008).
9. A. Salandrino and D. N. Christodoulides, "Airy plasmon: a nondiffracting surface wave," Opt. Lett. **35**(12), 2082–2084 (2010).
10. J. Broky, G. A. Siviloglou, A. Dogariu, and D. N. Christodoulides, "Self-healing properties of optical Airy beams," Opt. Express **16**(17), 12880–12891 (2008).
11. F. O. Fahrbach, P. Simon, and A. Rohrbach, "Microscopy with self-reconstructing beams," Nat. Photon. (2010).
12. A. Chong, W. H. Renninger, D. N. Christodoulides, and F. W. Wise, "Airy-Bessel wave packets as versatile linear light bullets," Nat. Photonics **4**(2), 103–106 (2010).
13. G. P. Agrawal and M. J. Potasek, "Nonlinear pulse distortion in single-mode optical fibers at the zero-dispersion wavelength," Phys. Rev. A **33**(3), 1765–1776 (1986).
14. D. Abdollahpour, S. Suntsov, D. G. Papazoglou, and S. Tzortzakis, "Spatiotemporal airy light bullets in the linear and nonlinear regimes," Phys. Rev. Lett. **105**(25), 253901 (2010).
15. D. G. Papazoglou, N. K. Efremidis, D. N. Christodoulides, and S. Tzortzakis, "Observation of abruptly autofocusing waves," Opt. Lett. **36**(10), 1842–1844 (2011).
16. R.-P. Chen, C.-F. Yin, X.-X. Chu, and H. Wang, "Effect of Kerr nonlinearity on an Airy beam," Phys. Rev. A **82**(4), 043832 (2010).

#151138 - $15.00 USD Received 14 Jul 2011; revised 3 Nov 2011; accepted 13 Nov 2011; published 30 Nov 2011

17. I. Kaminer, M. Segev, and D. N. Christodoulides, "Self-accelerating self-trapped optical beams," Phys. Rev. Lett. **106**(21), 213903 (2011).
18. Y. Fattal, A. Rudnick, and D. M. Marom, "Soliton shedding from Airy pulses in Kerr media," Opt. Express **19**(18), 17298–17307 (2011).
19. I. Dolev, T. Ellenbogen, and A. Arie, "Switching the acceleration direction of Airy beams by a nonlinear optical process," Opt. Lett. **35**(10), 1581–1583 (2010).
20. A. Bahabad, M. M. Murnane, and H. C. Kapteyn, "Manipulating nonlinear optical processes with acceperating light beams," Phys. Rev. A **84**(3), 033819 (2011).
21. V. E. Zakharov and A. B. Shabat, "Exact Theory Of Two-Dimensional Self-Focusing and One-Dimensional Self-Modulation Of Waves in Nonlinear media," Sov. Phys. JETP **34**, 62–69 (1972).
22. A. Hasegawa and F. Tappert, "Transmission of stationary nonlinear optical pulses in dispersive dielectric fibers. I. Anomalous dispersion," Appl. Phys. Lett. **23**(3), 142–144 (1973).
23. G. P. Agrawal, *Nonlinear Fiber Optics*, 3rd ed. (Academic Press, 2001)
24. G. I. Stegeman and M. Segev, "Optical Spatial Solitons and Their Interactions: Universality and Diversity," Science **286**(5444), 1518–1523 (1999).
25. J. R. Taylor, *Optical Solitons Theory and Experiment* (Cambridge Univ. Press, 1992).
26. H. A. Haus and W. S. Wong, "Solitons in optical communications," Rev. Mod. Phys. **68**(2), 423–444 (1996).
27. E. Iannone, F. Matera, A. Mecozzi, and M. Settembre, *Nonlinear Optical Communication Networks* (Wiley, 1998).
28. J. P. Gordon, "Interaction forces among solitons in optical fibers," Opt. Lett. **8**(11), 596–598 (1983).
29. F. M. Mitschke and L. F. Mollenauer, "Experimental observation of interaction forces between solitons in optical fibers," Opt. Lett. **12**(5), 355–357 (1987).
30. L. F. Mollenauer, S. G. Evangelides, and J. P. Gordon, "Wavelength Division Multiplexing with Solitons in Ultra-Long Distance Transmission Using Lumped Amplifiers," J. Lightwave Technol. **9**(3), 362–367 (1991).
31. A. Hasegawa and Y. Kodama, "Amplification and reshaping of optical solitons in a glass fiber-I," Opt. Lett. **7**(6), 285–287 (1982).
32. H. A. Haus, F. I. Khatri, W. S. Wong, E. P. Ippen, and K. R. Tamura, "Interaction of Solitons with Sinusoidal Wave Packet," IEEE J. Quantum Electron. **32**(6), 917–924 (1996).
33. H. A. Haus, W. S. Wong, and F. I. Khatri, "Continuum generation by perturbation of Soliton," J. Opt. Soc. Am. B **14**(2), 304–313 (1997).
34. Q. H. Park and H. J. Shin, "Parametric Control of Soliton Light Traffic by cw Traffic Light," Phys. Rev. Lett. **82**(22), 4432–4435 (1999).
35. H. J. Shin, "Soliton scattering from a finite cnoidal wave train in a fiber," Phys. Rev. E **63**(2), 026606 (2001).
36. H. J. Shin, "Interaction of a soliton with a continuous wave packet," Phys. Rev. E **67**(1), 017602 (2003).
37. E. A. Kuznetsov, A. V. Mikhailov, and I. A. Shimokhin, "Nonlinear interaction of solitons and radiation," Physica D **87**(1-4), 201–215 (1995).
38. E. A. Kuznetson and A. V. Mikhailov, "Relaxation oscillations of solitons," Pis'ma Z. Eksp. Teor. Fiz. **60**, 466–470 (1994).
39. J. Satsuma and N. Yajima, "Initial Value Problems of One-Dimensional Self-Modulation of Nonlinear Waves in Dispersive Media," Suppl. Prog. Theor. Phys. **55,** 284-306 (1974).
40. A. V. Buryak and V. V. Steblina, "Soliton collisions in bulk quadratic media: comprehensive analytical and numerical study," J. Opt. Soc. Am. B **16**(2), 245–255 (1999).
41. C. Simos, V. Couderc, A. Barthélémy, and A. V. Buryak, "Phase-dependent interactions between three-wave spatial solitons in bulk quadratic media," J. Opt. Soc. Am. B **20**(10), 2133–2141 (2003).
42. T. G. Philbin, C. Kuklewicz, S. Robertson, S. Hill, F. König, and U. Leonhardt, "Fiber-optical analog of the event horizon," Science **319**(5868), 1367–1370 (2008).
43. C. Yeh and L. Bergman, "Pulse shepherding in nonlinear fiber optics," J. Appl. Phys. **80**(6), 3174–3178 (1996).

1. Introduction

Airy wave packets were first introduced in the context of quantum mechanics as a curiosity [1], exhibiting a solution to the Schrödinger equation which both maintains its form and continuously accelerates, in opposition to conventional wisdom. However, such Airy beams, as well as Bessel beams which share the former distortionless property, are not physically realizeable as these beams contain infinite energy. Truncation of Bessel beams has long been a strategy for utilizing so-called non-diffracting beams [2,3], yet this solution has not been applied to Airy beams until recently [4–6]. These truncated Airy beams are experimentally easy to create, by applying a cubic phase mask across a Gaussian beam in the Fourier plane, and maintain the unique attributes of acceleration and self-similarity over an extended propagation range (eventually succumbing to diffraction). These unique attributes and experimental ease have sparked much interest as applicable to several fields of study and are now the topic of research for many research groups. Spatially truncated Airy beams have been applied in creating curved plasma channels [7], particle clearing [8], plasmonic energy

#151138 - $15.00 USD Received 14 Jul 2011; revised 3 Nov 2011; accepted 13 Nov 2011; published 30 Nov 2011

routing [9], and are capable of recovering from spatial obscurations due to their energy redistribution mechanism [10], making them useful for imaging in scattering media [11].

Since the spatial diffraction equation of light and the temporal dispersive equation are isomorphic, the attributes of spatial Airy beams can be directly translated to temporal Airy pulses. Such truncated Airy pulses are produced by impressing a cubic spectral phase onto an incident pulse by either pulse shaping techniques [12] or propagation in cubic dispersive media (at the zero dispersion wavelength) [13]. The resulting Airy pulse can propagate further without broadening in quadratic dispersive media (normal or anomalous), leading to spatially and temporally confined pulses or light bullets [12,14]. Airy pulses can be engineered to collide in time and space, resulting in significant peak power enhancements [15].

In the presence of optical nonlineaties, such as the intensity dependent Kerr effect, the Airy waveform is no longer an analytic solution of the Nonlinear Schrödinger equation (NLSE). The main Airy lobe, where the peak power is the highest, experiences greater amount of self-phase modulation leading to self-focusing or trapping. At relatively low powers, this enables the Airy beam to propagate further [16], and as powers increase the formation and shedding of solitons and even multiple-solitons can be observed [17]. Identical soliton shedding behavior has been observed for Airy pulses in the time domain [18]. Airy beams can also be created and switched by parametric processes in engineered quasi-phase-matched (QPM) media [19], and fine Airy spatiotemporal control in high-harmonic generation can be obtained in QPM structures [20]. While Airy beams/pulses do not maintain their shape in the presence of an optical potential created by the Kerr effect, solitons do. Solitons are an analytic, stable solution to the nonlinear Schrödinger equation [21–23], and consist of a self-similar yet non-accelerating beam (or pulse), balancing self-focusing against diffraction (or dispersion). Solitons have been extensively studied in both the spatial [24] and temporal domains [25], the latter out of interest for application in optical communications [26,27]. These studies have included soliton interactions, both coherent [21,28,29] (interactions between successive pulses in a bit stream) and incoherent [27,30] (collisions between pulses of different wave division multiplexing (WDM) channels, due to group velocity mismatch), and soliton perturbations from the stable solution [31–39]. These collision and perturbation effects play a decisive role in establishing the limit of soliton-based optical communications [27]. Research of spatial solitons in $\chi^{(3)}$ media, with coherent and incoherent light, and collisions and interaction between spatial solitons have also been investigated [24]. Interestingly, spatial solitons and interactions are also supported in $\chi^{(2)}$ media, by coupled waves via parametric processes [40,41].

In this work, we are interested in investigating the interactions between weak Airy pulses, which propagate according to the linear medium characteristics as their peak power is low, and stable soliton pulses at the same carrier frequency. We place them in proximity to each other, yet initially non-overlapping, with the Airy acceleration direction towards the soliton. Since the soliton is a stationary pulse, the weak accelerating Airy pulse propagates towards the soliton and begins interacting with it. We are interested to study whether the soliton will behave as an impenetrable barrier (as an event horizon) [42]—or rather analogously a shepherding pulse [43]—or whether the Airy probe can control the soliton propagation parameters [34], or as a collision perturbation [32], albeit the Airy can potentially have infinite energy (if non-truncated).

2. Airy-soliton interactions

The Airy-soliton interactions can be analyzed in either the spatial or temporal domain. We choose to perform the analysis in the temporal, due to a reduction of a spatial degree of freedom, making the analysis easier and faster to perform. However, any conclusions derived in the temporal domain can be applied to the spatial domain. Temporal waveform evolution is governed by the NLSE, expressed here in normalized coordinates [23]

#151138 - $15.00 USD Received 14 Jul 2011; revised 3 Nov 2011; accepted 13 Nov 2011; published 30 Nov 2011

$$i\frac{\partial u}{\partial \xi}+\frac{1}{2}\frac{\partial^2 u}{\partial \tau^2}+|u|^2 u=0 \tag{1}$$

where ξ and τ are the propagation distance and retarded time coordinates. Before proceeding to the interaction study, we review first the fundamental soliton and Airy pulse characteristics.

2.1 Temporal Airy pulse definition

Truncated temporal Airy pulses can propagate in a dispersive media, such as a single mode optical fiber, with a ballistic wavefront trajectory, but with respect to a retarded time frame, and remain quite resilient to dispersion effects when propagating in the linear regime (under low intensity). In the linear regime (dropping the potential term of Eq. (1), an input Airy pulse defined by $u_A(\xi=0,\tau)=\mathrm{Airy}(\tau)\exp(a\tau)$ evolves as:

$$u_A(\xi,\tau)=\mathrm{Airy}\left[\tau-\left(\frac{\xi}{2}\right)^2-ia\xi\right]\exp\left[a\tau-\frac{a\xi^2}{2}\right]\exp\left[i\left(+\frac{\xi^3}{12}-\frac{\left(a^2+\tau\right)\xi}{2}\right)\right] \tag{2}$$

where τ is the normalized retarded time variable, defined as $\tau=t-\xi/v_g$ (*t* is the lab time, and v_g is the group velocity at the carrier frequency), ξ is the normalized distance variable and *a* is the truncation coefficient (the signs of the imaginary terms are opposite to those in references [4–6] to ensure that for a positive quadratic dispersion coefficient we will have normal dispersion due to a sign difference between the paraxial equation found in references [4–6] and the dispersion equation found in [23]). In Eq. (2) the Airy function's argument has quadratic dependence on ξ which gives rise to the ballistic trajectory property. Figure 1(a) shows an intensity plot for the nonlinear propagation of a truncated Airy pulse in an anomalous dispersion fiber with zero loss and low peak intensity to propagate in the quasi-linear regime. To demonstrate the resilience to dispersion [12], Gaussian pulses travel $\sqrt{3}\,L_d$ (where L_d is the dispersion length) before the peak intensity is reduced by half, whereas an Airy pulse can travel several dispersion lengths; for example, an Airy pulse with a = 0.05 (0.005) truncation coefficient can propagate $5.5L_d$ (*16.7* L_d) before the peak intensity is reduced by half.

2.2 Temporal soliton pulse definition

The NLSE (Eq. (1) supports the well known fundamental soliton solution. For an initial condition: $u_S(\xi=0,\tau)=\mathrm{sech}(\tau)$, the propagated field is described by:

$$u_S(\xi,\tau)=\mathrm{sech}(\tau)\exp\left(i\xi/2\right) \tag{3}$$

which is stationary and self-similar in propagation (Fig. 1b).

#151138 - $15.00 USD Received 14 Jul 2011; revised 3 Nov 2011; accepted 13 Nov 2011; published 30 Nov 2011

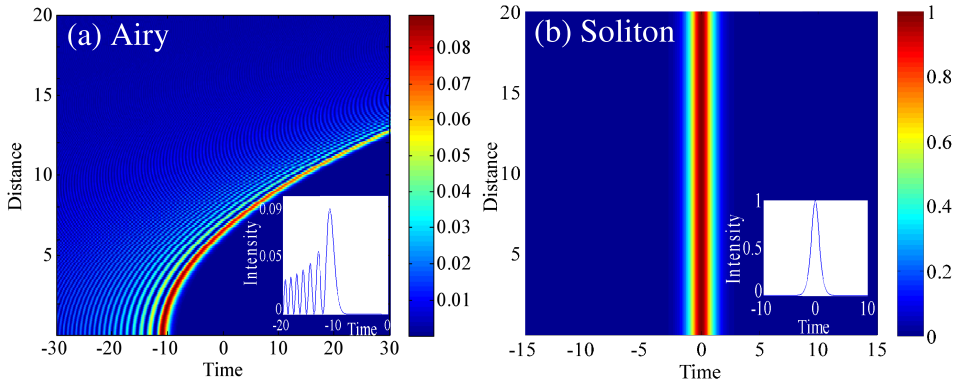

Fig. 1. Intensity plots for nonlinear propagation of (a) a weak truncated Airy pulse (*a* = *0.005*), and (b) a normalized Soliton both to *20* L_d. Insets show launched intensity distributions.

2.3 Airy-soliton interactions

The unique ballistic propagation feature of the Airy pulse gives it the ability to accelerate or decelerate (depending on the tail direction) and allows for interactions (collisions) between pulses having the same center frequency. By positioning the Airy pulse at a time separation away from the soliton, enables the Airy with the ballistic path to cross and interact with the soliton. We demonstrated these interactions through numerical simulations using the Split Step Fourier Method (SSFM) with a time window of 1300 time units divided to 32768 sampling points, and propagated to a distance of 100 soliton periods (157L_d units, where L_d = 1 in the normalized NLSE) with 1500 output inspection distances (not to be confused with the SSFM simulation step size which is less then one thousandth of L_d). Insight from the well known soliton-soliton [21,23,28,29] and soliton-continuous wave (CW) [31,34–36] interactions is applied to better understand the observed phenomena. From soliton perturbation theory, it is known that the perturbing pulse relative phase, amplitude (or total energy), initial time separation and frequency offset (difference in group velocities) play a role in the outcome of the interaction; thus in our simulations we vary these initial parameters of the perturbing Airy pulse to take them into consideration. Moreover, the perturbations affect the fundamental soliton parameters, namely the soliton phase, time position, amplitude and frequency. Consequently the launched initial conditions are (Fig. 2a):

$$u(\xi=0,\tau)=\operatorname{sech}\left(\tau\right)+r\,\mathrm{Airy}(\tau-\tau_0)\exp(a\left(\tau-\tau_0\right))\exp\left(i\theta\right) \tag{4}$$

The varied parameters in Eq. (4) are the amplitude ratio r between the Airy pulse and the soliton (normalized), the initial Airy time position τ_0 with respect to the soliton (launched at zero), and the relative phase θ of the Airy pulse. We choose r such that at the point of collision the peak intensity ratios between the accelerated Airy lobe and the soliton will be *8*, *4*, *2*, 1 and *0.5* percent (note that the Airy peak intensity at collision is already attenuated with respect to launched conditions on account of the truncation and dispersive propagation). These low Airy interference values ensure that the Airy will propagate in the quasi-linear regime and can be treated as a perturbation of the soliton [32]. The minimal time separation of $\tau_0 = -6$ is chosen to achieve at least a −30dB dip between the Airy and soliton at our time sampling (Fig. 2b), to ensure essenitially no initial overlap and interaction. We also choose a small enough truncation coefficient (*a* = *0.005*), which guarantees that the peak collision intensity of the Airy launched at our largest separation ($\tau_0 = -10$) will not be less then *95%* of that launched at the smallest separation ($\tau_0 = -6$) for every chosen launched amplitude. Hence all the Airy pulses have the same energy for a given r value and only a small variation in peak intensity at the point of collision.

#151138 - $15.00 USD Received 14 Jul 2011; revised 3 Nov 2011; accepted 13 Nov 2011; published 30 Nov 2011

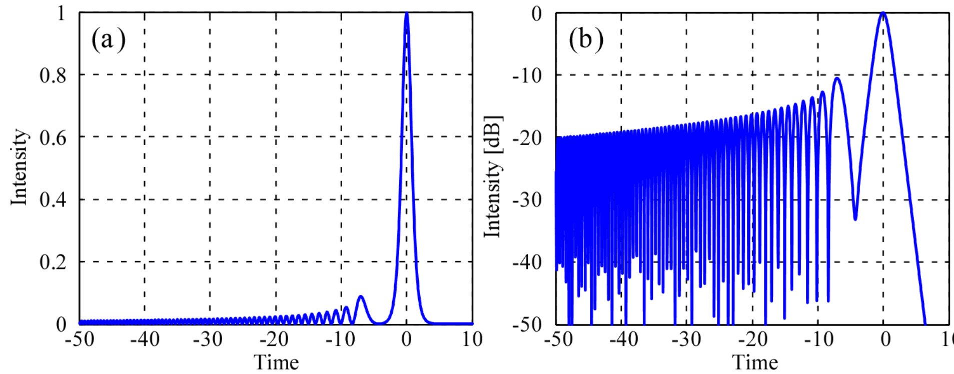

Fig. 2. Exemplary initial launch conditions composed of both the Airy ($a = 0.005$, 8% intensity at collision, $\tau_0 = -6$) and the normalized Soliton. (a) linear scale, (b) dB scale (the variation in dip values is an artifact of the sampling).

3. Simulation results

Exemplary Airy-soliton interactions are shown in Fig. 3, launched at a time separation of 10 time units ($\tau_0 = -10$) and an intensity ratio of 8% for two relative phases (0 and π). The propagating Airy decelerates (wavefront moves to later time) to collide with the trailing soliton pulse. The collision distance is given by:

$$\xi = \sqrt{4(\tau_{Soliton} - \tau_0 + \tau_{peak\ off\ set})} \tag{5}$$

where $\tau_{Soliton}$ is the soliton time position (in our case $\tau_{Soliton} = 0$) and $\tau_{peak\ offset}$ is the offset of the main Airy peak with respect to the Airy delay time τ_0 ($\tau_{peak\ offset}$ is numerically calculated for a given truncation, e.g. $\tau_{peak\ offset} \approx 1.014$ for $a = 0.005$). The interaction can be separated to two regimes of interest: the primary collision region between the pulses (occurring at approximately $3<\xi<15$, for our selected initial time separations), responsible for the main variation in the fundamental soliton parameters of phase, amplitude, frequency and time position, and a relaxation region accompanied by continuous interaction with the dispersed Airy tail (occurring at $\xi>15$). During the primary collision ($3<\xi<15$) both pulses lose their identities and cannot be distinguished [35] due to interference throughout the collision region [37]; however as the Airy wavefront moves towards later times the pulses reform and emerge having perturbed parameters. Since the truncated Airy pulse has the same center frequency and must maintain its first moment, it never completely crosses over the soliton; however the wavefront consisting of the main lobe, which has been designed to maintain its identity within the collision range, and subsequent lobes, do cross the soliton. (The Airy with our truncation coefficient of $a = 0.005$ was designed to decay to half peak power at $\xi = 16.7$, beyond the collision zone.) Therefore, the Airy-soliton interactions are classified as *incomplete collisions*, defined as having either an initial temporal overlap or a terminal overlap after the collision (the latter occurring in our case), as opposed to *complete collisions*, (i.e. full crossing of the pulses achievable through non overlapping bandwidths and GVD [27,32,35]). These complete collisions, as present in WDM collisions, are known to be independent of relative phase and do not undergo a permanent frequency change after collision. Consequently, our findings show that the soliton undergoes a permanent frequency shift in some cases (Fig. 4 demonstrates the most extreme case for $\tau_0 = -6$), and that the interaction (and frequency shift) is strongly dependent on relative phase, as in coherent soliton-soliton [23,27] and soliton-CW [31] interactions.

#151138 - $15.00 USD Received 14 Jul 2011; revised 3 Nov 2011; accepted 13 Nov 2011; published 30 Nov 2011

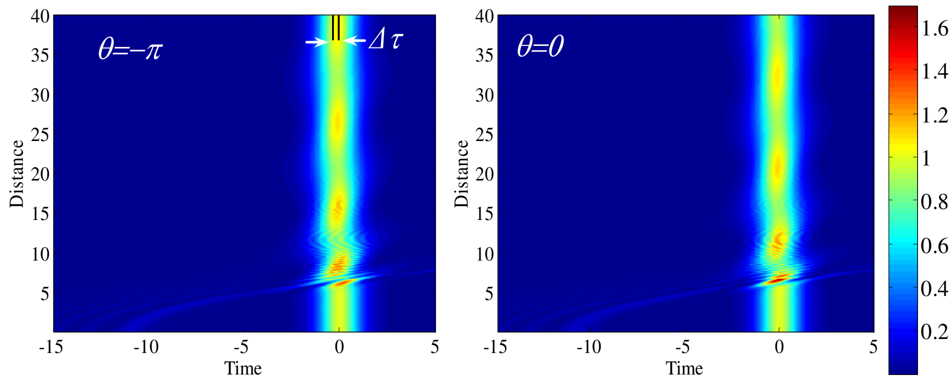

Fig. 3. Airy-Soliton interactions with an initial separation of 10 and intensity ratio of 8% at collision for two phases. (a) $\theta = -\pi$, (b) $\theta = 0$

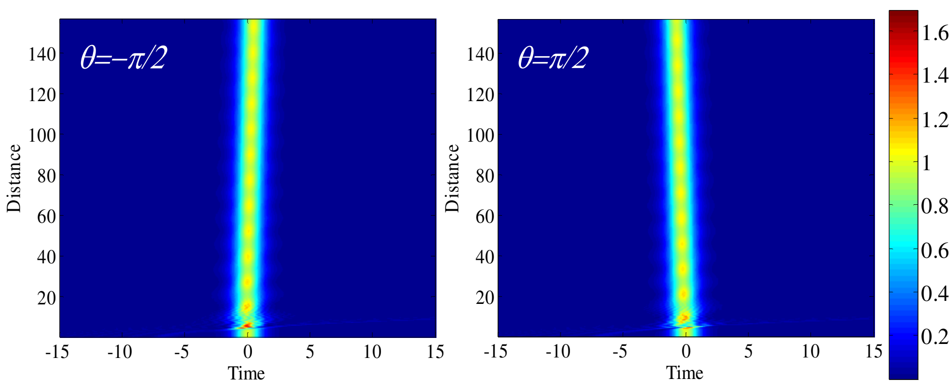

Fig. 4. Airy-Soliton interaction with $\tau_0 = -6$ and 8% intensity ratio showing a permanent frequency change when (a) $\theta = -\pi/2$, and (b) $\theta = \pi/2$ over $157\ L_d$ units (100 soliton periods).

An analysis of soliton-soliton collisions in WDM systems and coherent soliton interactions is carried in [27], offering an explanation for the dependence on relative phase or the lack of it based on perturbation theory developed by Haus *et. al.* [32,33]. The derivation distinguishes between coherent and non-coherent interaction. For example, soliton-soliton collisions in a WDM system are regarded as incoherent interactions. The perturbation term taken into account in this case is only the cross phase modulation (XPM); the remaining terms originating from the NLSE nonlinear response are neglected due to rapid beating that average out to zero [27]. However, in the coherent derivation (i.e. soliton-soliton coherent interactions) the beat term between the two waveforms is taken into consideration.

Our investigative case bears similarity to coherent interactions at times, especially pronounced at closer initial separation while at other times the interaction is more incoherent in nature, when the initial separation is large and the spectral repositioning by dispersion results in interaction between waveforms with a reduced spectral overlap. This distinction can be better understood by observing the Airy pulse evolution in time-frequency space as a function of propagation distance. Figure 5 shows the spectrogram (time-frequency space) of an evolving Airy pulse at different propagation distances (which basically shears the Airy spectrogram), demonstrating the spectral repositioning and the amount of spectral overlap of the colliding wavefront with the soliton. (The soliton's stationary time-frequency signature is denoted by the green ellipse.) A more significant spectral overlap between soliton and Airy at point of collision is observed for an initial separation of $\tau_0 = -6$ (compare middle column spectrograms in Fig. 5). Upon further propagation, the soliton propagates with quasi-CW light background from the dispersed Airy, demonstrated by the spectral overlap found in the right column in Fig. 5. As the propagation distance grows this dispersed background radiation becomes more monochromatic and approaches the same carrier frequency as the soliton. The continuous interaction results in oscillations of the solitons frequency and amplitude and therefore both the time position and phase will oscillate and gradually decay [31].

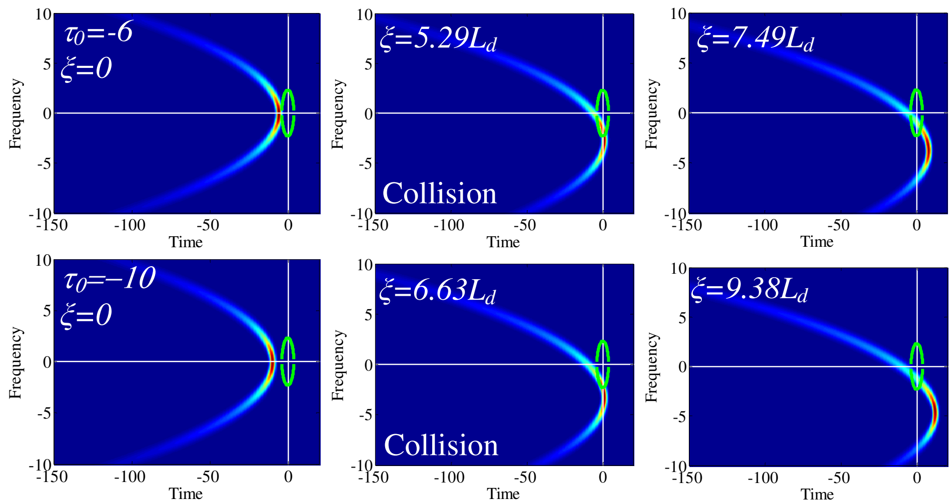

Fig. 5. Spectrogram of the Airy pulse at three selected distances for two initial separations; upper row: $\tau_0 = -6$, lower row: $\tau_0 = -10$. Left column: launch condition, center column: at collision distance (*5.29* L_d units and *6.63*, respectively), right column: at distance where Airy wavefront is at a temporal shift of twice the initial time separation (*7.49* L_d units and *9.38*, respectively). Green ellipse denotes the Soliton extent over time and frequency.

4. Analysis

To better quantify the simulation results from Figures such as 3 and 4, we track the soliton fundamental parameters from the SSFM results. The launched soliton prior to collision ($\xi<3$) and the perturbed emergent soliton ($\xi>15$) can be identified from the simulation results. However, during the collision event we cannot extract any useful information throughout, as the soliton is indistinguishable.

We extract the emergent soliton characteristics from the numerical results and not resort to the well-developed perturbation theory analysis, as the Airy-soliton interaction case is incomplete. Perturbation theory analysis requires the interaction to be complete and that the perturbation spectrum not exceed that of the soliton, neither of which holds for our Airy-soliton pulse case.

To derive high resolution emergent soliton parameters devoid of sampling effects, we locate the intensity peak at each propagation distance, select a sufficient number of intensity samples around the peak value, and then apply a sech(•)^2 intensity profile fit to the selected samples. The fit quality is excellent. The benefit of this procedure is that it allows us to construct a continuous soliton intensity profile with respect to time at a given distance, from which we extract the intensity, time position, and temporal width at high resolution and with no discretization effects. This procedure generates smoothly varying curves for the fundamental soliton parameters' evolution. (The soliton phase is directly extracted from the field sample with the strongest peak intensity.)

#151138 - $15.00 USD Received 14 Jul 2011; revised 3 Nov 2011; accepted 13 Nov 2011; published 30 Nov 2011

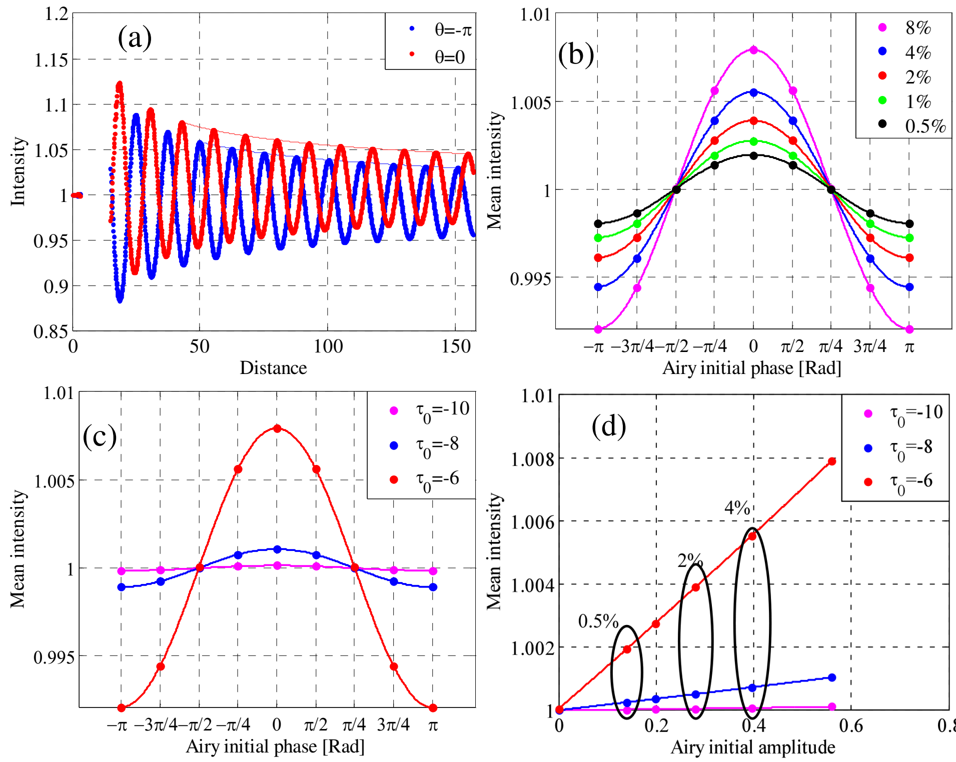

Fig. 6. Soliton intensity oscillations. (a) Intensity oscillation (intensity ratio of 8% and $\tau_0 = -6$). Also shown envelope fit of the form $1/\sqrt{z}$, (b) Mean intensity of the oscillations with a sinusoidal fit, (c) dependence with respect to the Airy's initial phase for all the time separations (intensity ratio of 8%), (d) Mean intensity for all separations with at *8%* intensity ratio for the $\theta = 0$, (with a second order polynomial fit; behavior predominantly linear) .

Soliton power

The soliton peak power behavior is analyzed along the propagation range and is charted in Fig. 6a for the closest Airy-soliton separation ($\tau_0 = -6$), highest Airy power (*8%*) and for two representative relative phases ($0, \pi$). The emergent soliton exhibits peak power oscillations that are dependent on the colliding Airy pulse phase. We further see that the two curves are vertically displaced, indicating a different mean soliton intensity (both oscillate nearly about the launched (original) soliton peak power). We next chart the mean peak soliton intensity for different initial Airy phases and launched powers at $\tau_0 = -6$ (see Fig. 6b). (The mean soliton intensity is calculated far from collision, by establishing soliton power and background power from the maximum and minimum interference values. These interferences are due to the soliton's natural SPM.) We observe sinusoidal dependence on the initial Airy phase for all powers, indicating an energy transfer between the pulses during the primary collision [33]. Similar sinusoidal behavior is observed at larger time separations (i.e., $\tau_0 = -8$ and $\tau_0 = -10$), albeit at a lesser magnitude (Fig. 6c shows mean intensity fluctuation only at the 8% collision intensity for clarity). Since the overall colliding energy is the same, regardless of initial time separation (i.e., all energy contained in the Airy's delayed lower frequency components), the less pronounced effect at larger initial separations demonstrates that with greater time separation a more incoherent collision between soliton and the Airy occurs due to a larger frequency offset at collision event (as previously explained by spectrograms). For the largest time separation we find that the mean intensity is nearly unchanged, while for the shortest time separation the mean intensity is predominantly linearly dependent on Airy amplitude.

#151138 - $15.00 USD Received 14 Jul 2011; revised 3 Nov 2011; accepted 13 Nov 2011; published 30 Nov 2011

This linear relationship between mean soliton energy change and perturbation amplitude is another indication of coherent interaction behavior (Fig. 6d).

We also see the intensity oscillations decay in magnitude along the propagation as the soliton relaxes. The functional form of the decay is in agreement with [37–39] that states that within the region of the asymptotic solution the non-soliton part decays as $\xi^{-1/2}$ (Fig. 6a). The period between oscillations varies slightly from one oscillation to another (on account of the dispersed Airy background center frequency approaching that of the soliton), converging towards a constant period of 4π distance units (corresponding to the distance over which a soliton accumulates 2π phase), as the soliton propagates away from the collision region. The beating comes from the interference between the soliton SPM with the dispersed, now quasi-CW, Airy background.

Soliton time position and center frequency

We next track the soliton change in time position (e.g. Figure 3, $\theta = -\pi$). Solitons experience time position change through local frequency changes during the collision and permanent frequency changes which map to time position alterations by group velocity dispersion (GVD) [26,33–36]. Figure 7 plots the soliton time shift for several phases at collision with 8% Airy pulses for each of the three investigated time separations ($\tau_0 = -6, -8, -10$). The most prominent feature is a soliton permanent frequency change after the main collision, which occurs after the collision with the Airy's wavefront and is much more pronounced at closer initial time separations. The frequency change is also strongly dependent on relative phase between the Airy and soliton, and can be positive or negative (soliton travels slower or faster, respectively). As the propagation progresses, the time shift oscillates about the time shift induced solely by the permanent frequency change. These oscillations are attributed again to the ongoing propagation through the dispersed Airy and are dependent on its amplitude and frequency detuning [31]. All solitons also experience a discrete time shift after the primary collision, which appears weakly dependent on the initial time separation and phase.

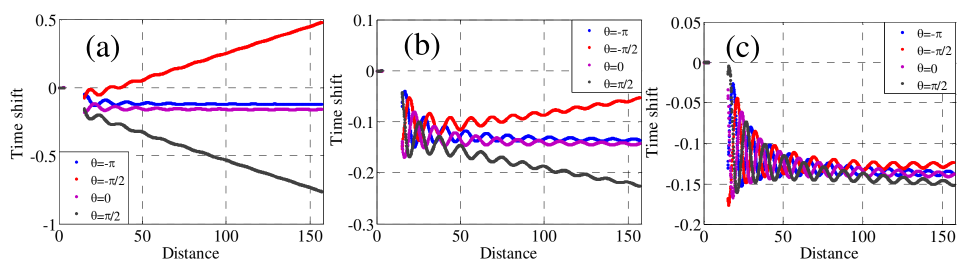

Fig. 7. Soliton time shift for all initial separations with an 8% intensity ratio for selected phases. (a) $\tau_0 = -6$, (b) $\tau_0 = -8$, (c) $t_0 = -10$. Note that the scale of the time shift is not identical in all three cases.

We find the permanent frequency change experienced by the soliton by applying a linear fit to each trace in Fig. 7 (the fit is performed from about mid propagation distance up the end), where the slope represents the frequency change. The frequency change is dramatically stronger for closer time separations (Fig. 8a, for $\theta = -\pi/2$ at which a large positive frequency change is observed for all separations), while for larger separations the frequency change eventually disappears. This behavior is in line with our previous finding that at small initial separations the collision has coherent interaction characteristics, while for larger separations the collision is incoherent (exhibiting no permanent frequency change). This conclusion is supported by the linear dependence on Airy amplitude for the closest time separation ($\tau_0 = -6$). The permanent frequency change is also sinusoidally dependent on the Airy phase (Fig. 8b).

#151138 - $15.00 USD Received 14 Jul 2011; revised 3 Nov 2011; accepted 13 Nov 2011; published 30 Nov 2011

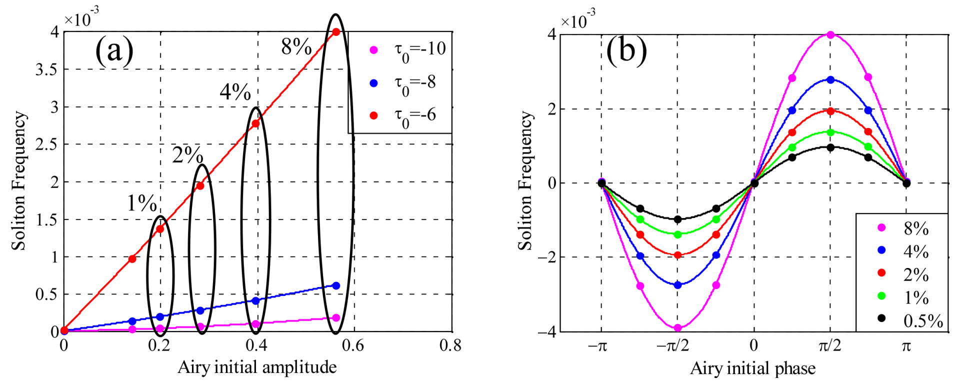

Fig. 8. (a) Soliton frequency change with respect to amplitude at $\theta = \pi/2$, (b) Sinusoidal fit with respect to Airy phase for amplitudes with $\tau_0 = -6$ of the frequency change.

We plot the soliton discrete time shifts after the primary collision for all separations at different Airy intensities and its weak phase dependence in Fig. 9. The time shifts are all negative (towards the Airy wavefront) as in complete collisions [27,32,36], depend quadratically on the Airy's initial amplitude with little dependence on initial separation (Fig. 8a), and are hardly dependent on Airy initial phase (Fig. 8b). This behavior bears the signature of complete collisions with the main and subsequent lobes [27,32]. To obtain an estimate for the discrete time shift generated by the primary collision (which is within the collision zone, hence masked by interference), we use the linear fit lines for the soliton time position (previously used to measure the frequency change) calculated at the collision distances given by Eq. (5) for each initial time separation case. Hence, the primary collision results in a nearly fixed discrete time shift for the soliton and bears the signature of complete collision, while the soliton acquires a permanent frequency change during the same collision for close Airy launch (coherent collision characteristic, due to the spectral overlap at collision).

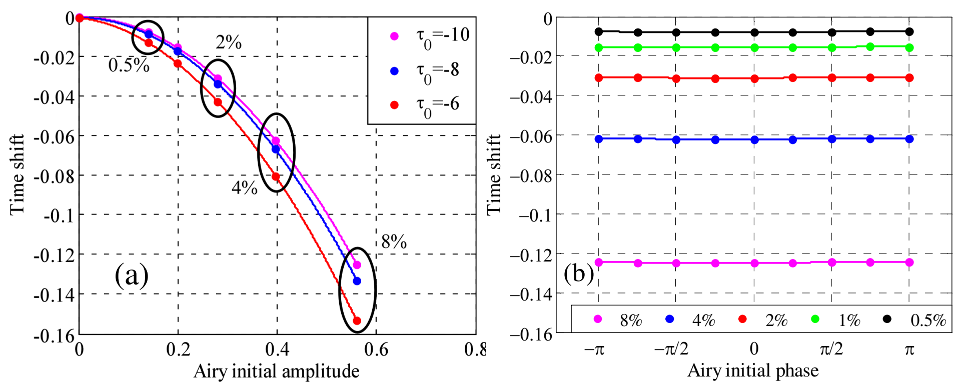

Fig. 9. Estimated time shift form, (a) Time shift with respect to Airy's initial amplitude for all initial time separations ($\theta = 0$), Time shift with respect to Airy's initial phase and amplitude with $\tau_0 = -10$ and a sinusoidal fit profile .

Soliton phase

The last emergent soliton parameter we follow is the phase. Solitons continuously acquire phase along the propagation distance, and we subtract this constant term in all our results (using the launched soliton parameters) so that we only witness the phase difference between that of the expected phase of the unperturbed soliton and that of emergent soliton (see Fig. 10 for 8% Airy intensity for all the separations and select phases). As in the time shift results (Fig. 7), we see a discrete phase offset after the primary collision, in all cases equaling about

#151138 - $15.00 USD Received 14 Jul 2011; revised 3 Nov 2011; accepted 13 Nov 2011; published 30 Nov 2011

0.2 radians, and divergent and oscillatory phase in the relaxation region. While the oscillatory behavior is explained by the continuous interaction with the dispersed Airy background radiation (resultant of local intensity and frequency oscillations), the linear component is a reflection of the emergent soliton perturbed parameters of mean intensity and center frequency. Both terms contribute to the accumulated phase linearly with respect to ξ and quadratically on the amplitude and frequency changes of the soliton [27]. For example, in Fig. 10a we see that for the initial phases of $\theta = -\pi$ and $\theta = 0$ there is a linearly-dependent phase difference attributed solely to a change in mean intensity, as the emergent soliton had only a mean intensity change (see Fig. 6b) and no permanent frequency change (see Fig. 8b) for these launched conditions. (A change of approximately 0.4 radian is accumulated between distances of 50 to 150, which translates to mean intensity change of approximately 0.008, exactly as found in Fig. 6b). In addition, we find that for the case of $\theta = -\pi/2$ and $\theta = \pi/2$ the small change in frequency of approximately 4×10^{-3} results in a negligible change since the phase term is quadratically dependent on frequency change.

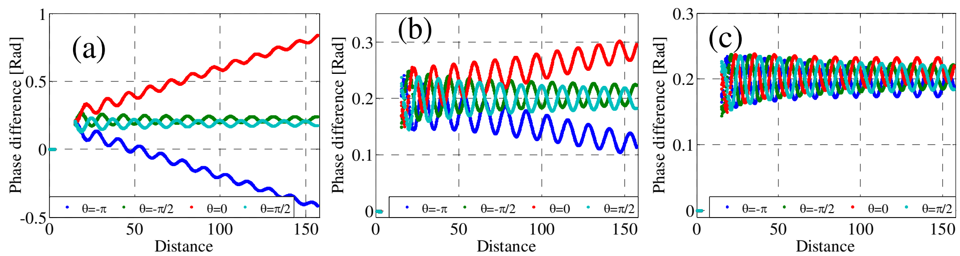

Fig. 10. Phase difference along the Airy propagation for select Airy initial phases with an intensity ratio of *8%* (a) $\tau_0 = -6$, (b) $\tau_0 = -8$, (c) $\tau_0 = -10$.

5. Conclusions

We have demonstrated the unique attributes of the interaction between a colliding Airy pulse and a soliton pulse at the same center frequency through split-step Fourier method simulations. The interactions are made possible by the ballistic trajectory property of the Airy pulse.

Our findings show that the interactions are described by two regions of propagation. The first region, at which the primary collision occurs with the intense main lobe of the Airy wavefront, is responsible for the main change of the soliton fundamental parameters. The nature of the interaction at the primary collision is strongly dependent on the initial Airy-soliton time separation, varying from coherent to incoherent interaction. At closer separations, the collision event is accompanied by spectral overlap between the Airy and soliton and the resulting coherent interaction perturbs the soliton frequency and amplitude. At larger initial time separation, the interaction is incoherent as there is decreasing spectral overlap and the rapidly oscillating phase of the interference term does not accumulate to significant frequency and amplitude changes. In both cases, however, the soliton does experience a discrete time and phase change, due to a complete collision with the Airy main lobe. The second region of propagation is beyond the collision event, which is primarily defined by continuous interactions with the dispersed Airy tail, resulting in oscillations of the time shift and phase through local intensity and amplitude changes respectively. The soliton experience slow relaxation throughout this secondary region, as the Airy disperses and the oscillations' magnitude diminishes.

The nature of the interactions that were simulated are of collisions. In all cases, the Airy pulse propagated through the soliton pulse. This is in contrast to an intense soliton acting as an event horizon that can block the Airy pulse propagation [42]. An interesting future research effort could be to investigate the conditions leading to a soliton barrier, by possibly choosing a more intense and shorter duration soliton. In our simulations the Airy bandwidth exceeds that of the soliton, emphasizing the effect of dispersion.

While we performed all our analysis in one dimensional temporal media, i.e. dispersive and nonlinear fiber propagation, all our findings should hold in one and two dimensional spatial propagation cases in Kerr media as the underlying equations defining the interactions are isomorphic.

#151138 - $15.00 USD Received 14 Jul 2011; revised 3 Nov 2011; accepted 13 Nov 2011; published 30 Nov 2011